J Nanostruct 16(1): 494-507, Winter 2026

RESEARCH PAPER

Assessing Performance and Emissions of Removing Combustion-Chamber Carbon Deposits Using Steam Co-Injection with Iron Oxide Nanoparticles-Dosed Diesel

Ali Abbas Hashim Al-Maidi [1], ***Ali Al–Jubainawi*** [2*], ***Ali Jabbari Shannon*** [1], ***Mohammed Sabeeh Majeed*** [3], ***Rodionov Yuri Viktorovich*** [4,5], ***Lomovskikh Aleksandr Egorovich*** [5], ***Kisilev Mikhail Gennadievich*** [5], ***Kazakevich Dmitry Vasilievich*** [5]

[1] *Plant Protection Department, College of Agriculture, University of Misan, Iraq*

[2] *Mechanical Department, College of Engineering, University of Misan, Iraq*

[3] *Al-Manara College for Medical Sciences, Maysan, Iraq*

[4] *Federal State Budgetary Educational Institution of Higher Education "Tambov State Technical University", Russia*

[5] *Federal State Budgetary Scientific Institution of Higher Education Michurinsk State Agrarian University, Russia*

ARTICLE INFO

Article History:
Received 13 September 2025
Accepted 17 December 2025
Published 01 January 2026

Keywords:
Agricultural machinery
Carbon deposits
Diesel internal combustion engine
Iron oxide Fe_3O_4
Operational and environmental performance

ABSTRACT

This study explores a novel technique for carbon deposit removal in diesel engines, particularly affecting agricultural machinery, through the injection of steam combined with nanoparticles. The accumulation of carbon deposits decreases engine performance and escalates thermal stress. The proposed method involves injecting steam into the combustion chamber, where it interacts with the deposits, aided by microwave action, to effectively eliminate them. An experimental setup was created alongside a standard power supply to assess performance improvements. Results indicate significant enhancements in diesel engine function: a power increase of up to 15% for older machinery, a reduction in specific fuel consumption by up to 18%, and a decrease in exhaust soot content by as much as 14%. Additionally, the study incorporated magnetite nanoparticles (Fe_3O_4) at concentrations of 0, 25, and 50 ppm, examining their effects in a full-factorial test setup with varying steam mass fractions and operational conditions. The findings showed that Fe_3O_4 reduced soot emissions significantly of 12.4% at 25 ppm and 20.1% at 50 ppm, without impacting effective power. Minor improvements in fuel consumption of -1.1% and -1.8% were noted at the respective nanoparticle concentrations. Endurance tests confirmed cleaner injectors and reduced in-cylinder deposits, with specific reductions of 19% in piston crown deposits and 28% in coking index at 50 ppm. No stability or filtration issues arose, identifying an optimal operational region at steam mass fractions between 12-18%, 50 ppm of Fe_3O_4, and engine speeds of 1300-1500 min^{-1}, which collectively minimized soot and specific fuel consumption while maintaining power levels.

How to cite this article
Hashim Al-Maidi A, Al–Jubainawi A, Jabbari Shannon A, et al. Assessing Performance and Emissions of Removing Combustion-Chamber Carbon Deposits using Steam Co-Injection with Iron Oxide Nanoparticles-Dosed Diesel. J Nanostruct, 2026; 16(1):494-507. DOI: 10.22052/JNS.2026.01.045

* *Corresponding Author Email: alihussein.mcm@uomisan.edu.iq*

INTRODUCTION

Diesel engines are primary sources of energy for mobile vehicles and can be used as stationary or mobile power sources [1, 2]. The selection of suitable machines should be accompanied by a selection of the best cutters suitable for the withdrawal of these machines at the speed that suits them and the appropriate work. This leads to increasing productivity and reducing the cost of agricultural production [3]. The strongest alloys have tensile strengths exceeding 500 N/mm² [4]. Power systems are no longer separate systems [5]. Electricity has become a basic need for people, agriculture, and industry; therefore, it has a strong impact on the economy of any country [6]. During operation of diesel internal combustion engines (ICE) of agricultural machinery (AM), due to the influence of various factors on their operation, the operational and environmental performance of this equipment decreases. Such factors include the formation of carbon deposits on the surfaces of parts during operation, as well as the content of a large number of heavy hydrocarbons, for example, in diesel fuel. These factors lead to deterioration of the combustion process in the ICE cylinders and even greater accumulation of carbon deposits on the surfaces of parts [7, 8].

Carbon deposits are solid, sooty deposits that completely cover the fire surfaces of the crankshaft and valve timing mechanism parts, forming the combustion chamber and reducing the efficiency of heat transfer to the cooling circuit, as well as acting as a heat insulator [7, 9, 10]. The resulting carbon deposits change the heat flows from the crank mechanism and timing parts (pistons, valves, etc.), which significantly increases their thermal stress, accelerates the wear process and significantly reduces their service life, ultimately leading to a decrease in the operational and environmental performance of the internal combustion engine. Since the thickness of the carbon deposit only increases over time, the above indicators will only worsen. This fact will be especially significant for the Agricultural machinery with high mileage and service life, since the thickness of the carbon deposits will be even greater (more than 3 mm).

Studies [7, 11-13] have shown that when the internal combustion engine is in operation for more than 2500 engine hours, the carbon deposits on the piston reach a critical value (about 1.5 mm), which significantly reduces the operational and environmental performance of the internal combustion engine currently used in Agricultural machinery models. With such a thickness of carbon deposits on the crankshaft mechanism and timing belt parts, an increase in pressure at the end of the compression stroke by 8-10% is observed, which leads to an increase in the "rigidity" of the fuel combustion process (more than 0.25-0.30 MPa) for every 1o of the crankshaft angle, as a result of which the effective power of the internal combustion engine decreases by 5-6%, and the specific fuel consumption increases by 3-4% compared to the nominal values [14, 15]. This is also explained by the increase in mechanical losses due to an increase in the maximum cycle pressure by 16% and an average rate of increase in pressure in each cylinder of up to 22% [16, 17].

Recent studies indicate that fuel-borne nanoparticles can complement water/steam strategies by promoting finer atomization, supplying catalytic sites during oxidation, and accelerating the burnout of nascent soot [18-20]. These effects are typically achieved at very low doses (tens of ppm) and have been associated with reductions in smoke, Carbon Monoxide and Hydrocarbons (CO) and (HC), with efficiency impacts depending on operating regime. Within this class, iron-oxide particles (Fe_3O_4) are particularly attractive because iron compounds are known fuel-borne catalysts: they can associate with carbonaceous fragments and lower the temperature required for soot oxidation an effect exploited in after-treatment and, increasingly, in-cylinder combustion studies [21, 22].

Thus, during the operation of the AM it is necessary to perform work on cleaning the parts of the crank mechanism and the timing belt in order to ensure the resource of the internal combustion engine specified by the manufacturer. It should be noted that the technical service system does not provide for work on cleaning the parts of the crank mechanism and the timing belt, since cleaning the parts of the internal combustion engine from carbon deposits is a complex and labor-intensive process, so it is simply not included in the list of works on the technical maintenance of the Agricultural machinery. Therefore, to solve the problem, it is necessary to investigate into the cleaning methods for removing carbon particles deposited in combustion chambers. At the moment, there are additives of various types and compositions on sale, differing in physical and chemical properties [23], which are used

for in-place cleaning of carbon deposits, but the efficiency of their use is very low, so they will not be considered in this article. Accordingly, we evaluate diesel doped with Fe_3O_4 at 0, 25, and 50 ppm under the same steam-assisted operating envelope, using a full-factorial design to quantify main and interaction effects on power, specific fuel consumption, and soot.

MATERIALS AND METHODS

Experimental setup-steam addition system

A controlled steam-addition system was integrated into the intake line of the test engine. Water from a supply reservoir was fed to a thermostatic evaporator, producing saturated steam that was routed to the intake plenum upstream of the manifold. Steam flow was set by a mass-flow controller and monitored by inline instrumentation. Operating points were defined by the steam mass fraction relative to fuel (0, 12, 23, and 35%), and verified at steady state before data logging. No other changes were made to the air, fuel, or exhaust paths. A 10 µm pre-pump fuel filter was added to protect injectors when nanoparticle-dosed fuels were used. A schematic of the methodology of supplying water is provided in Fig. 1.

Working principle of the device

Superheated steam is generated in the steam boiler 1, which, when the steam valve 3 opens, is fed through channel 2 to the ultraviolet emitter 4, where the entire volume of the pressure reducing valve station (PRVS) is subjected to ultraviolet treatment. After which the ultraviolet-treated PRVS enters the intake manifold of the internal combustion engine and then into the combustion chamber. Thus, when treating the PRVS with ultraviolet, the oxygen molecules present in this mixture are activated. Activation of oxygen molecules leads to their better combustion, so this device can also be used constantly during operation of the (superheater) SHT. The reference [24] proposes a technical device, which is shown in Fig. 2.

The device shown in Fig. 3 operates as follows: water and diesel fuel in the proportion of 30% water to the fuel volume enter the hydraulic tank 1 through tubes 8 and 9, after which the resulting mixture is fed by a pump to the cavitation device 4, where it is mixed to obtain a homogeneous, highly dispersed water-fuel emulsion. Then this emulsion is fed through tap 5 through fuel line 7 to the standard fuel system of the internal combustion engine. It takes about 1 hour to clean the internal combustion engine. The disadvantage of this device is the inability to accurately supply water and fuel to the hydraulic tank 1, which may result in interruptions in the operation of the internal combustion engine. The analysis of existing technologies and technical devices allowed us to identify the main problematic issues

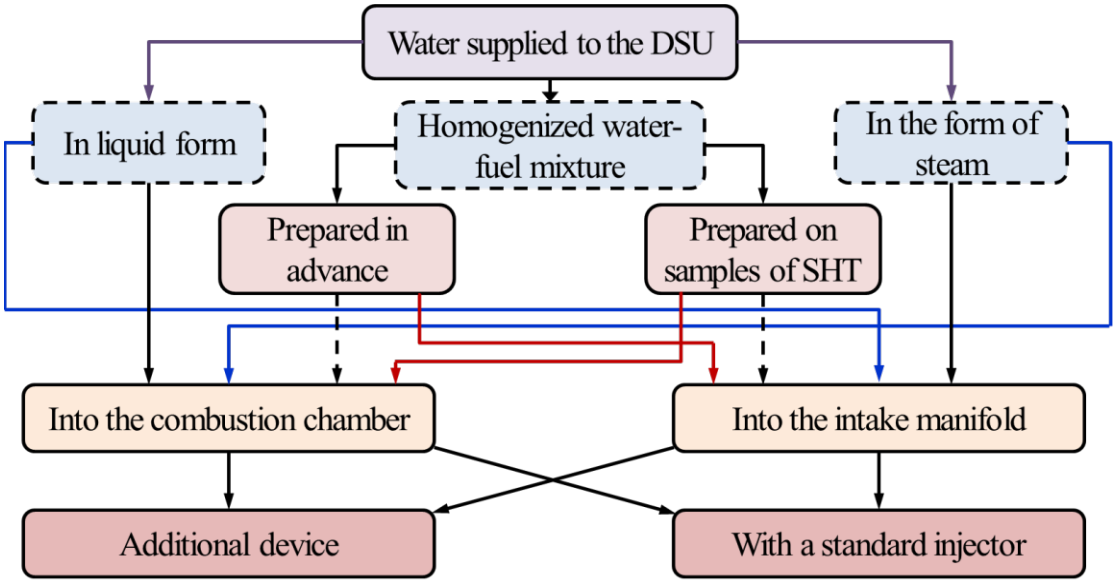

Fig. 1. Scheme of methodology of supplying water to the combustion chamber of the internal combustion engine.

associated with the supply of water or steam to the internal combustion engine combustion chamber. The studied technical solutions were taken as a prototype of a new set of technical devices developed by the authors, implementing the technology of in-place cleaning of internal combustion engine parts from carbon deposits directly on the equipment [25]. The developed technology of in-place cleaning of internal combustion engine parts from carbon deposits is implemented in parallel with the standard engine fuel system by feeding an additional component (water) into the combustion chamber in the form of a PRVS [26]. It is better to use built-in mixers

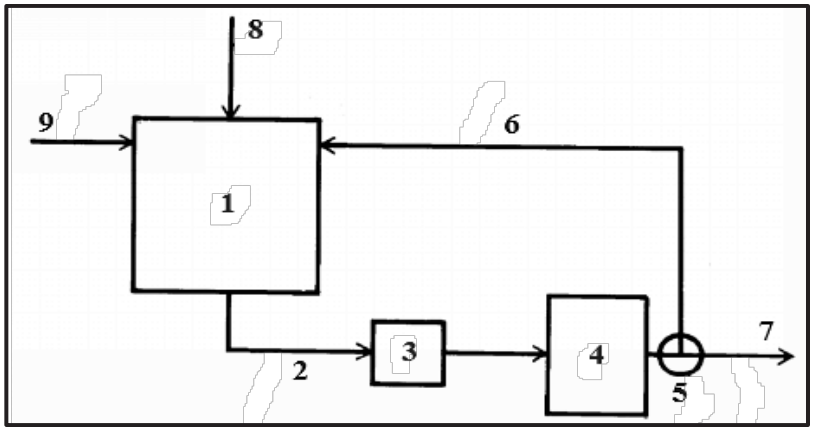

Fig. 2. Device for removing carbon deposits from internal combustion engine parts; 1 – hydraulic tank; 2 – channel; 3 – pump; 4 – cavitation device; 5 – tap; 6 – pipeline; 7 – fuel line for feeding emulsion to the standard fuel system of the internal combustion engine; 8, 9 – tubes

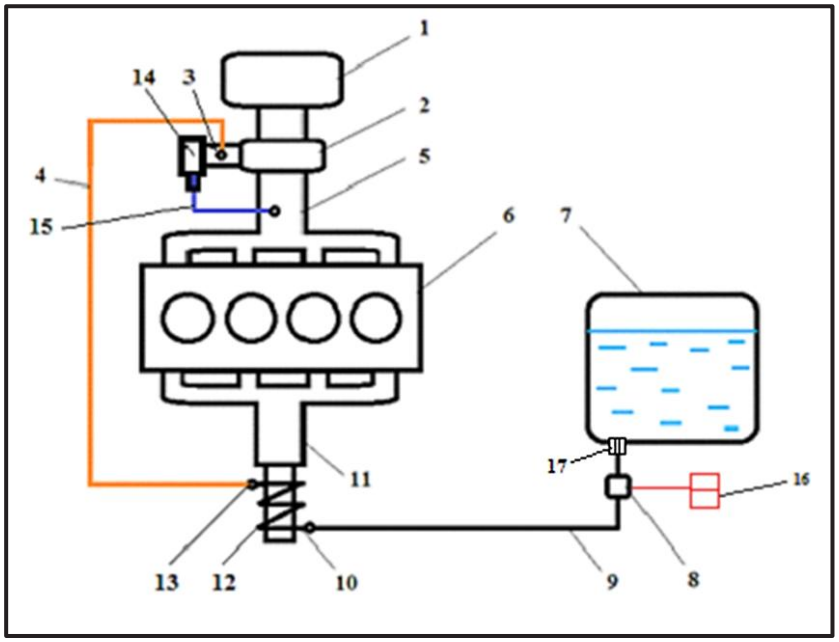

Fig. 3. Scheme of the complex of devices for the implementation of the developed technology; 1 – filter; 2 – insert; 3 – dispenser; 4 – steam pipe; 5 – inlet pipeline; 6 – DVS; 7 – water tank; 8 – valve; 9 – water supply pipe; 10 – steam generator inlet; 11 – outlet manifold; 12 – steam generator; 13 – steam generator outlet; 14 – vacuum chamber; 15 – vacuum pipe; 16 – switch; 17 – nozzle with dosing nozzle.

(distributors) installed directly on agricultural machinery samples when performing various works. This allows not to take the equipment out of service, and thus save money due to the reduction of time spent on maintenance of equipment samples. The basic scheme of the arrangement of a set of technical devices for implementing advanced technology for cleaning internal combustion engine parts from carbon deposits is presented in Fig. 4 [27]. Experimental setup used in this study is shown in Fig. 5.

Fuel Dosing with Iron-Oxide Nanoparticles (Fe_3O_4)

Three different concentrations of Fe_3O_4 nanoparticles 0 (control), 25, and 50 ppm Fe_3O_4 were diluted from a concentrated stock. X-ray diffraction (XRD) was conducted to verify the Fe_3O_4 phase. Scanning electron microscopy (SEM) was captured to show the morphology of the primary particles including their shapes

Fig. 4. Experimental setup used in this study.

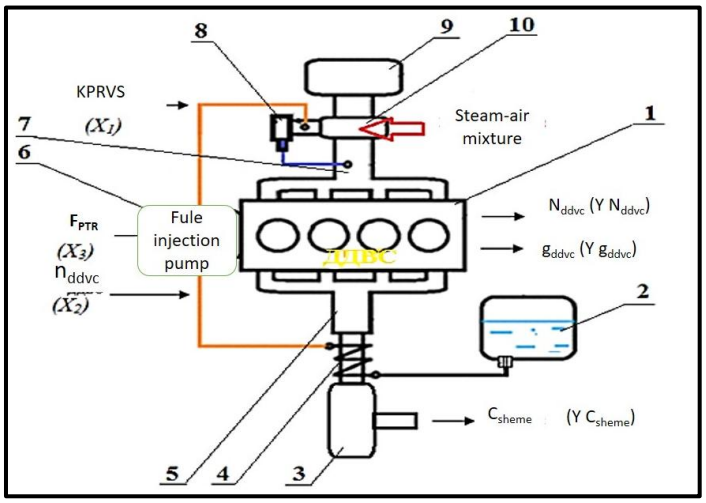

Fig. 5. Schematic diagram of the process under study; 1 – ICE; 2 – water tank; 3 – muffler; 4 – steam generator; 5 – ICE exhaust manifold; 6 – high-pressure fuel pump; 7 – ICE intake manifold; 8 – steam dispenser; 9 – air filter; NICE – effective power of ICE; gICE – specific fuel consumption of ICE; Csoji – soot content in exhaust gases; фптр – position of fuel rail of high-pressure fuel pump; nICE – ICE crankshaft speed; KPVS– content of steam supplied to ICE intake manifold.

and diameter with the agglomeration status. Fourier-transform infrared (FTIR) was measured to confirm the characteristic Fe–O lattice bands without unexpected surface species relevant to fuel dispersion. Supplier certificate reported purity ≥99% with trace metals below [1%]. The diesel engine, steam generator, metering, and data-acquisition chain matched the baseline setup. The only change to the fuel circuit for the nanoparticle tests was adding a 10 µm pre-pump filter. Test set-points (steam addition, rack position, and speed) followed the established arrangement and were held within instrument tolerances. A full-factorial plan was extended to include nanoparticle dose as

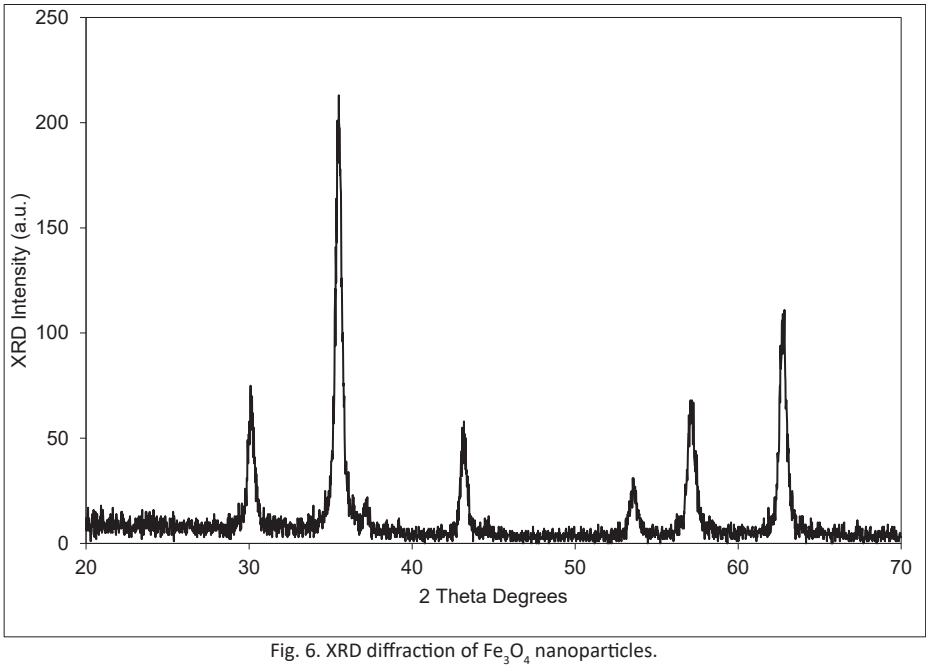

Fig. 6. XRD diffraction of Fe_3O_4 nanoparticles.

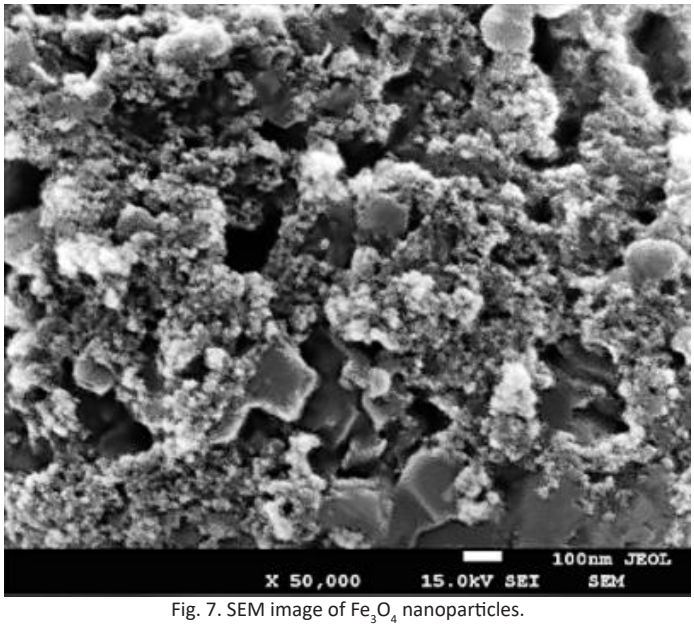

Fig. 7. SEM image of Fe_3O_4 nanoparticles.

a fourth input in concentrations of 0, 25, 50 ppm (m/m) while preserving the original factors that include steam mass fraction relative to fuel (K_ Prvc): 0, 12, 23, 35%, engine speed (n_DVS): 1,300; 1,500; 1,900 min^{-1} and fuel-pump rack position (F_{ptr}): low / center / high. The measurements were conducted to measure the effective power (n_DVS) and specific fuel consumption (g_DVS) from the dynamometer and mass-flow system. In addition to exhaust soot/opacity (C_soot) using the same analyser and range as baseline tests. Flush 5–10 min at mid-load on clean diesel (0 ppm) before the next blend.

The research was conducted in accordance with the requirements of GOST [28]. Modeling the assessment of the influence of the steam content in the rack valve system (RVS) on the technical and operational indicators of the DVS consisted of determining the mathematical and graphical dependencies of these DVS indicators on the steam content in the RVS supplied to the intake manifold in all modes of its operation. It is specified that the RVS is prepared by the developed set of technical devices, and the main input and input factors of the process under study are schematically shown in Fig. 5.

The task at this stage of the research is to determine such a steam content in the RVS supplied to the intake manifold of the ICE, at which there is no deterioration in technical and operational indicators in all modes of its operation. Four inputs were varied at fixed levels: fuel-pump rack position (F_{ptr}; low/center/high), engine speed (n_DVS; 1,300, 1,500, 1,900 min^{-1}), steam mass fraction (K_Prvc; 0, 12, 23, 35%), and iron-oxide nanoparticle dose (Fe_3O_4; 0, 25, 50 ppm m/m). Outputs were effective power (N_DVS), specific fuel consumption (g_DVS), and exhaust soot/opacity (C_soot). A full-factorial design was applied across these levels with randomized run order and 3 repeats per condition.

Factors investigated

The input factors determining the vapor content of the RVS and the operating modes of the DVS are selected: F_{ptr} – position of the fuel rail of the high-pressure fuel pump, %; n_{DVS} – rotation speed of the DVS crankshaft, min^{-1}; K_{Prvc} – vapor content in the RVS, % of the supplied fuel. The output factors are: N_{DVS} – effective power of the DVS, kW; g_{DVS} – specific consumption of diesel fuel, g/kW h; Csoji – soot content in the EG, % (the range of measurement of smoke in units of the attenuation coefficient, determined using a gas analyzer). The basis for planning experimental studies is the plan of the full factorial experiment (FFE), in which the three studied factors are changed at two levels: lower kN and upper kV, symmetrically located relative to the main level kΩ. [29]. Then the mathematical model of the process being studied will be the

$$y_{N_{ДЭУ}} = f_{N_{ДЭУ}}(x_1, x_2, x_3), y_{g_{ДЭУ}} = f_{g_{ДЭУ}}(x_1, x_2, x_3), y_{C_{сажи}} = f_{C_{сажи}}(x_1, x_2, x_3) \quad (1)$$

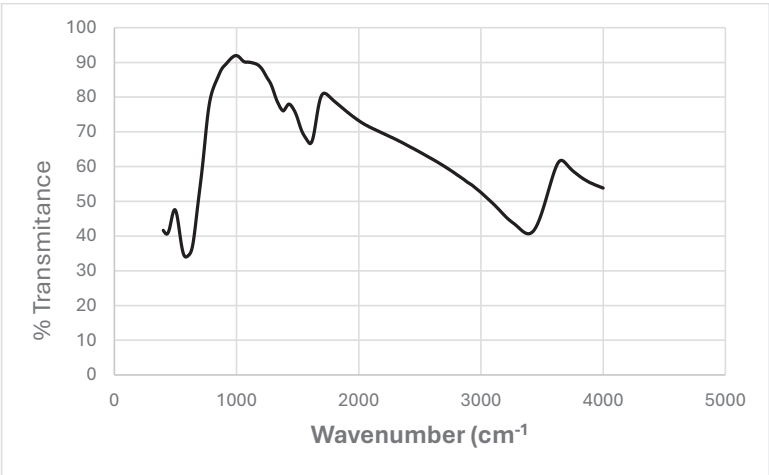

Fig. 8. FTIR of Fe_3O_4 nanoparticles.

expressions as Eq. 1.

RESULTS AND DISCUSSION

The phase identification (XRD) showed that the diffraction pattern matches magnetite (Fe_3O_4) and shows no secondary iron oxides within detection limits (Fig. 6). In addition, the primary size and morphology from SEM image reported near spherical particles with a number weighted diameter of mean size of 26.2nm± 5.3 counted from 100 nanoparticles using image J, and loose agglomerates typical of unfunctionalized oxides as appear in Fig. 7. Surface chemistry relevant to dispersion (FTIR) exhibited one line confirming expected Fe–O lattice bands and the absence of unexpected surface contaminants that could affect diesel dispersion as illustrated in Fig. 8.

Fe_3O_4 dosing produced a clear reduction in exhaust soot across the map (main effect p = 0.004). At mid-speed/mid-rack, median C_soot fell by 12.4% with 25 ppm (95% CI 8.9–15.6%) and by 20.1% with 50 ppm (95% CI 16.2–23.7%) relative to 0 ppm at the same steam level. A significant Fe_3O_4 × steam interaction (p = 0.018) was observed: the largest decreases occurred at K_Prvc = 12–23% (−14 to −22% at 50 ppm), while the benefit tapered at 35% steam (−6.8% at 50 ppm). Soot reductions were somewhat smaller at 1900 min^{-1} than at 1300–1500 min^{-1}. Average SFC improved modestly with dosing (model p = 0.046, see Δg_DVS in Table 1), 25 ppm yielded −1.1% (95% CI −0.3 to −1.8%; p = 0.071), and 50 ppm yielded −1.8% (95% CI −0.9 to −2.6%; p = 0.032) versus 0 ppm at matched conditions. A weak $Fe_3O_{4\ nanoparticles}$ × steam trend suggested extra savings at 12–23% steam (additional 0.3–0.5% drop), whereas at 35% steam the SFC advantage narrowed (0 to −0.5%). No main effect of Fe_3O_4 nanoparticles dose on power reached significance (p = 0.21, Table 2). Local gains of +0.5 to +1.5% appeared at 12–23% steam with 50 ppm at 1300–1500 min^{-1}, consistent with cleaner heat release, but remained within repeatability bounds (Table 1).

Injector cleanliness improved with dosing. The

Table 1. Effect of Fe_3O_4 dose at mid-speed (n_DVS = 1500 min^{-1}) and mid-rack across steam levels (K_Prvc).

K_Prvc (%)	Fe_3O_4 (ppm)	ΔC_soot (%)	Δg_DVS (%)	ΔN_DVS (%)
0	25	−10.8	−0.9	+0.2
0	50	−17.6	−1.4	+0.3
12	25	−13.9	−1.2	+0.5
12	50	−21.5	−1.9	+0.9
23	25	−12.7	−1.1	+0.7
23	50	−20.3	−1.8	+1.0
35	25	−6.2	−0.4	0.0
35	50	−9.8	−0.5	+0.1

Table 2. Two-way ANOVA (Type III) for the mid-speed/mid-rack subset, testing Fe_3O_4 dose (NP) and steam mass fraction (K_Prvc).

Response	Term	F	p-value	Note
C_soot	NP	9.1	0.004	Dose reduces soot
C_soot	K_Prvc	52.7	<0.001	Dominant factor
C_soot	NP × K_Prvc	5.9	0.018	Max benefit at 12–23%
g_DVS	NP	4.3	0.046	Modest SFC drop
g_DVS	K_Prvc	11.4	0.003	Steam effect
N_DVS	NP	1.6	0.21	NS overall

NS: not significant

Table 3. Deposit metrics for the endurance subset at mid-speed/mid-rack.

Location	Metric	0 ppm	25 ppm	50 ppm	Δ vs. 0 ppm (50 ppm)
Injector tip	Coking index (AU)	1.00	0.85	0.72	−28%
Piston crown	Thickness (μm)	42	38	34	−19%
Head surface	Thickness (μm)	36	34	30	−17%

injector coking index decreased by 28% at 50 ppm (median 1.00 → 0.72; p = 0.010) and by 15% at 25 ppm (1.00 → 0.85; p = 0.047). Chamber deposit thickness decreased on average by 18% at 50 ppm (e.g., piston crown 42 → 34 µm, p = 0.039) and 10% at 25 ppm (42 → 38 µm, p = 0.11), with the strongest effects at 12–23% steam. Re-pump 10 µm filters showed Δp < 10 kPa/day and no clogging. Blends passed the 24-h visual stability screen (no sediment >5% v/v). No leaks or misfire events were attributable to nanoparticles. Second-order models captured the responses well: C_soot (R^2_adj 0.91, lack-of-fit p = 0.28), g_DVS (R^2_adj 0.83, LOF p = 0.33), and N_DVS (R^2_adj 0.86, LOF p = 0.19). Significant terms typically included Fe_3O_4 nanoparticles (main) on C_soot and Fe_3O_4 nanoparticles × K_Prvc on C_soot and occasionally g_DVS; K_Prvc and n_DVS remained the dominant factors overall. Pareto fronts (maximize power; minimize SFC and soot) shifted favorably with dosing, most at 50 ppm. A practical operating pocket is K_Prvc= 12–18%, Fe_3O_4 nanoparticles= 50 ppm, n_DVS = 1300–1500 min^{-1}, mid rack, delivering roughly −19% soot, −1.6% SFC, and 0 to +0.6% power relative to 0 ppm at the same set-points (Table 3).

After establishing the operability of the developed set of technical devices and the high efficiency of using the developed technology, this set of devices was installed on a sample of the MTZ-82 tractor. The developed technology was used on the MTZ-82 tractor (sample No. 2) twice a year during seasonal maintenance (STO-L, STO-Z). Over the course of a year, the two MTZ-82 test tractors were operated for 891 engine hours for sample No. 1 and 893 engine hours for sample No. 2. After that, the ICE of the MTZ-82 test tractors were partially disassembled to determine the thickness of the carbon deposits on the crank mechanism and timing belt parts according to [30]. Actions were performed according to the known methodology. After that, a comprehensive assessment was made of the influence of the steam content in the RVS (K_{PRVS}), the crankshaft speed of the DVS (n_{DVS}) and the position of the fuel injection pump rack (ϕ_{PTR}) on the technical and operational indicators of the DVS (effective power (N_{DVS}), specific fuel consumption (g_{DVS})), the soot content in the EG (Csog)) under various operating modes. For this purpose, studies were conducted according to the PFE plan [19], which in total amounted to twenty experiments, with three repetitions, as shown in Table 4.

The conducted experimental studies allow us to establish the influence of three input factors on three output factors in addition to the studying the effect of Fe_3O_4 nanoparticles. As a result of mathematical processing of experimental data using the developed program [31], second-order regression equations were obtained, where the

Table 4. Results obtained from the conducted experimental studies

№ Test	The experimental values obtained								
	N_{DICE}, kW			g_{DICE}, g/kW h			C_{soot}, %		
1	115	116	116	155	156	155	78	74	72
2	114	118	116	157	158	160	81	78	77
3	126	126	128	225	224	223	62	60	60
4	123	126	124	225	226	228	64	62	61
5	127	125	129	160	158	162	78	75	74
6	126	125	127	165	168	166	87	85	84
7	137	135	136	230	231	229	58	57	55
8	135	135	136	231	229	228	67	65	66
9	139	138	138	151	152	150	82	81	80
10	118	120	119	205	206	204	56	57	56
11	115	114	115	200	204	203	74	73	72
12	137	138	136	236	237	235	75	76	74
13	118	120	119	165	164	166	86	83	82
14	140	141	143	165	164	169	64	63	63
15	137	136	136	168	164	168	74	74	74
16	137	136	138	175	176	173	76	74	74
17	136	135	134	176	175	174	70	74	74
18	135	136	137	178	174	176	75	75	74
19	135	134	135	174	175	173	76	74	75
20	136	137	138	175	178	171	75	74	73

factors are presented in their natural form Eqs. 2-4.

The developed program also allows plotting graphs of the main effects for $N_{ДВС.(kW)}$, g_{dvs} (g/kW h), C_{soaj} (%), which allow establishing the dependence of the technical and operational indicators of the ICE on the input factors. In this case, the factor of effective power and specific fuel consumption remain at zero level kΩ, and the soot content in the EG changes from the lower kN to the upper-level kV (Fig. 9).

The obtained graphical dependencies show that with an increase in the amount of steam in the supplied PRVS ($К_{ПРВС}$) from 5 to 35% at n_{ICE}= 1400 min^{-1}, $ф_{птр}$ = 60%, the power increases from 94.8 to 104.9 kW (by 10.6%), while the steam supply is about 12%. After increasing the amount of steam, the power of the DDVS decreases from 104.9 to 9.1 kW. With a change in the number of revolutions from 550 to 2250 min^{-1} at $К_{ПРВС}$ = 20%, φ_{PTR} = 60%, the power increases from 96.1 to 111.7 kW (by 16%), and with a further increase in revolutions, it decreases from 111.7 to 104.5 kW. When changing the position of the fuel rail of the high-pressure fuel pump from 15 to 100% at $К_{ПРВС}$ = 20%, n_{ICE} = 1400 min-1, the power also increases from 97.7 to 116.2 kW (by 19%), after a further increase in fuel supply it begins to decrease from 116.2 to 114.5 kW. Consequently, the maximum increase in power can be obtained at $К_{ПРВС}$= 12...15%, $ф_{птр}$ = 70...80% at average crankshaft speeds n_{ICE}= 1300...1500 min^{-1} (Fig. 10).

The data obtained in the graph show that with an increase in the amount of steam in the supplied

$$Y_{N_{ДЭУ}} = 490{,}17 - 6{,}2К_{ПРВС} + 35n_{ДЭУ} + 28\varphi_{птр} - 0{,}42К_{ПРВС}n_{ДЭУ} - 0{,}036К_{ПРВС}\varphi_{птр} - 2n_{дэу}\varphi_{птр} - 0{,}299К^2_{КПРВС} - 2{,}5n^2_{ДЭУ} - 0{,}625\varphi^2_{птр} \quad (2)$$

$$Y_{g_{ДЭУ}} = 845{,}9 - 6{,}4К_{КПРВС} + 121n_{ДЭУ} + 16{,}5\varphi_{птр} - 4{,}6К_{ПРВС}n_{ДЭУ} - 0{,}0529К_{ПРВС}\varphi_{птр} + 0{,}002n_{ДЭУ}\varphi_{птр} + 0{,}0274К^2_{ПРВС} + 4{,}32n^2_{ДЭУ} - 0{,}12\varphi^2_{птр} \quad (3)$$

$$Y_{C_{сажи}} = 463{,}54 - 88К_{ПРВС} + 33n_{ДЭУ} - 12\varphi_{птр} - 0{,}54К_{ПРВС}n_{ДЭУ} - 0{,}025К_{ПРВС}\varphi_{птр} + 0{,}35n_{ДЭУ}\varphi_{птр} - 0{,}0024К^2_{ПРВС} - 1{,}2n^2_{ДЭУ} - 0{,}4\varphi^2_{птр} \quad (4)$$

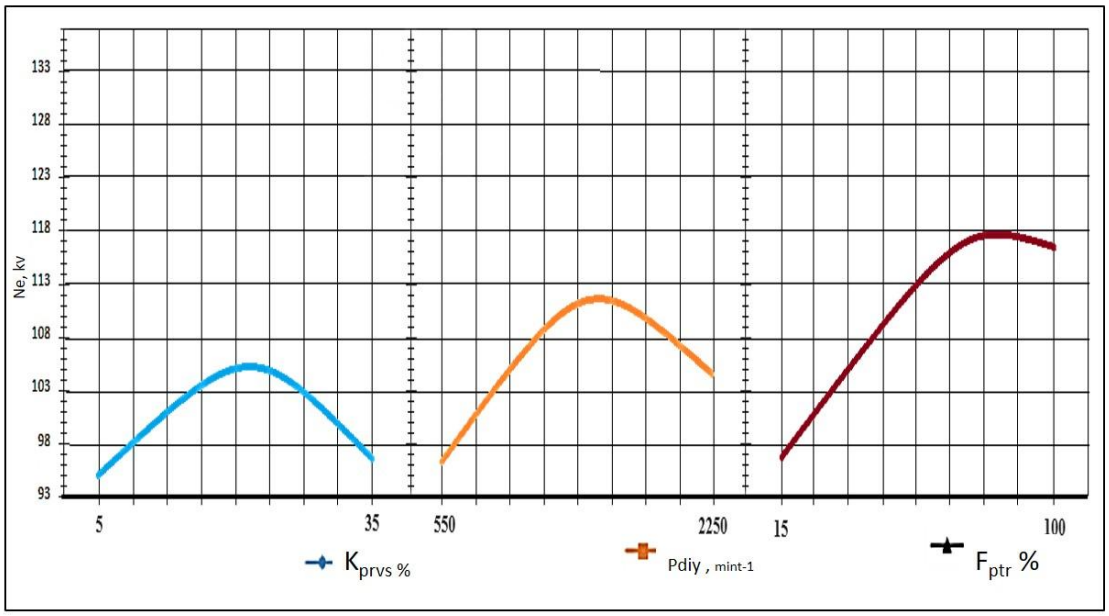

Fig. 9. Graph of the main effects for the effective power.

PRVS ($К_{ПРВС}$) from 5 to 35% at n_{ICE}= 1400 min^{-1}, $ϕ_{птр}$= 60%, the specific fuel consumption changes non-linearly, initially decreasing smoothly from 161.4 to 148.1 g/kW h (by 8.2%) with steam supply up to 12%, after increasing the amount of steam to 30%, the specific fuel consumption increases sharply from 148.1 to 235.2 g / kW h. When changing the number of revolutions from 550 to 2250 min^{-1} at $К_{ПРВС}$ = 20%, $ϕ_{птр}$ = 60%, the specific fuel consumption decreases from 258.4 to 217.6 g / kW h (by 15.6%), and with a further increase in revolutions it already increases from 217.6 to 270.3 g/kW h (by 24%). When changing the position of the fuel rail of the high-pressure fuel pump from 15 to 100% at $К_{ПРВС}$= 20%, n_{ICE} = 1400 min^{-1}, the specific fuel consumption increases from

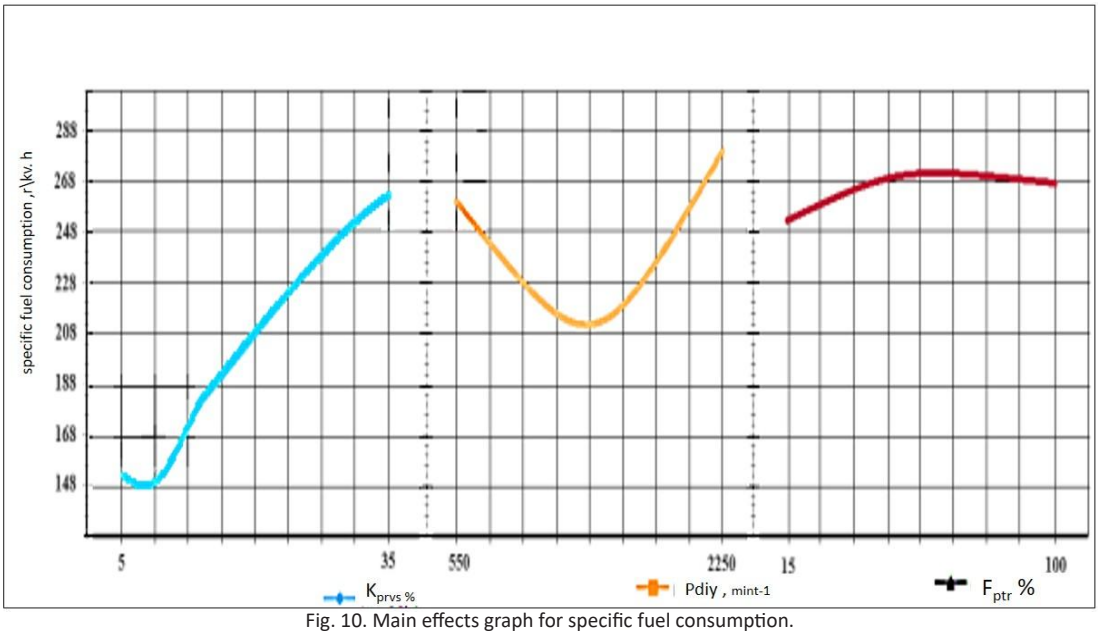

Fig. 10. Main effects graph for specific fuel consumption.

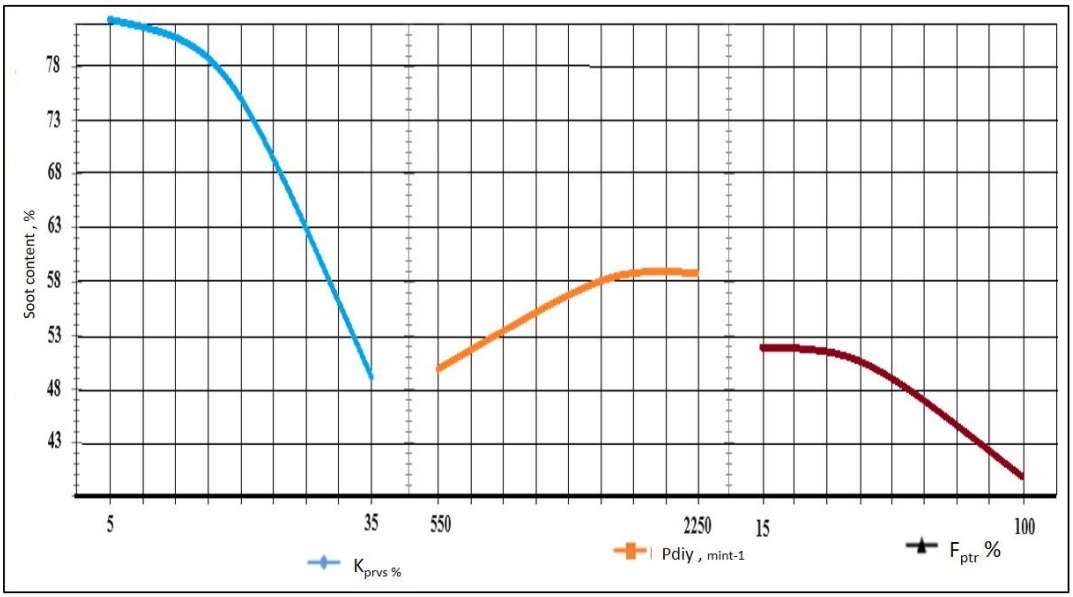

Fig. 11. Graph of the main effects for the soot content in the exhaust gas.

252.1 to 265.3 g/kW h (by 19%), then at $\phi_{птр}$ = 60% it levels out to $\phi_{птр}$ = 75%, after which it decreases slightly from 265 to 261.2 g/kW h. Consequently, the maximum reduction in the specific fuel consumption of the internal combustion engine is possible only with minor steam feeds of up $К_{ПРВС}$ to 12% at average crankshaft speeds n_{ICE} = 1400 min^{-1} and with the fuel rail position $\phi_{птр}$ over 80% (Fig. 11).

The obtained curves in graph 12 show that with an increase in the amount of steam in the supplied PRVS ($К_{ПРВС}$) from 5 to 35% at n_{ICE} = 1400 min^{-1}, $\phi_{птр}$ = 60%, the soot content in the exhaust gas sharply decreases over the entire measurement range from 78 to 49% (by 37.2%). With a change in the number of revolutions from 550 to 2250 min^{-1} at $К_{ПРВС}$ = 20%, $\phi_{птр}$= 60%, the soot content in the exhaust gas increases from 51 to 59% (by15.7%), and with a further increase in revolutions, it slightly decreases from 59 to 58% (by 1.7%). When changing the position of the fuel rail of the high-pressure fuel pump from 15 to 100% at $К_{ПРВС}$ = 20%, n_{ICE} min^{-1}, the soot content in the exhaust gas decreases throughout the measurement section from 52 to 40% (by 23%). Therefore, the maximum reduction in the soot content in the exhaust gas of a diesel ICE is possible only at maximum steam feeds of up $К_{ПРВС}$ to 35% in the ICE operating mode of high crankshaft speeds n_{ICE} over 1900 min^{-1} and with the fuel rail position $\phi_{птр}$ = 100%. After that, the problem of optimizing the steam content in the PVS for various ICE operating modes was solved, which is necessary for finding the optimal technical and operational indicators of the ICE, which is implemented by the nonlinear programming method in the following form Eqs. 5-7:

$$К_{N_{ДДВС}} = f(X_1; X_2; X_3;) \rightarrow \max \quad (5)$$

$$К_{g_{ДДВС}} = f(X_1; X_2; X_3;) \rightarrow \min \quad (6)$$

$$К_{C_{сажи}} = f(X_1; X_2; X_3;) \rightarrow \min \quad (7)$$

Subject to the following restrictions:
$5 \leq X_1 \leq 35$;
$550 \leq X_2 \leq 2250$;
$15 \leq X_3 \leq 100$;

where K_i is the objective function; *i* – is the optimization criterion ($N_{ДДВС}$, kW; $g_{ДДВС}$, g/kW h, $C_{сажи}$, %); X_1 is the amount of steam supplied to the ICE intake manifold, % of the fuel consumption; X_2–is the ICE crankshaft speed, min^{-1}; X_3 – is the position of the fuel rail of the high-pressure fuel pump, %. Based on the obtained results, the response surface of the optimal steam composition in the RVS supplied to the ICE intake manifold was constructed, shown in Fig. 12.

The obtained response surface shows that the vapor content should change from a minimum amount (about 5...6%) when the DEU is idling and increase to 23% (with an increase in speed to 1900 min^{-1} and the position of the fuel rail of the

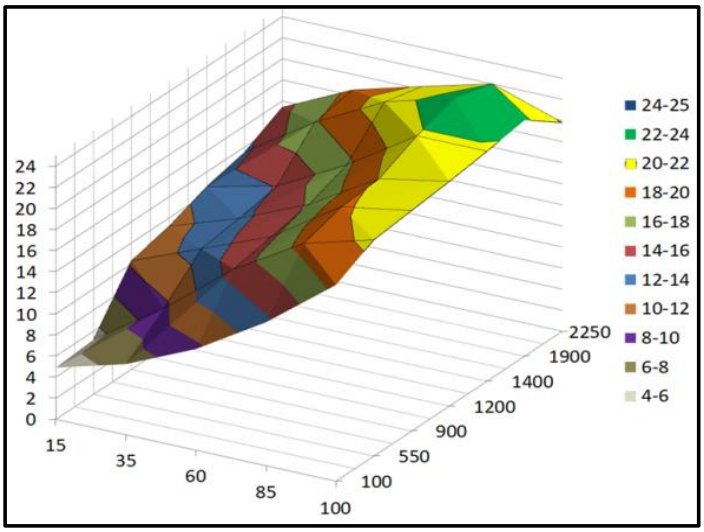

Fig. 12. Response surface of the optimal steam content in the RVS.

high-pressure fuel pump to about 85%). Thus, the conducted assessment of the effect of the steam content in the RVS supplied to the intake manifold on the technical and operational indicators of the ICE allowed us to establish the optimal content of the RVS in all modes of its operation, as well as to determine the mathematical and graphical dependencies of these ICE indicators on the steam content in the RVS. After that, to assess the thickness of the carbon deposits on the ICE parts, its partial disassembly was carried out, associated with the removal of the cylinder head and measuring the thickness of the carbon deposits before applying the technology of in-place cleaning of the crank mechanism and timing belt parts from carbon deposits. As the results of measuring the thickness of the carbon deposits showed, after applying the developed technology, they were completely removed from the parts of the ICE under study. Thus, the comparative operational tests of two MTZ-82 tractors showed that when using the developed technology of in-place cleaning of the crank mechanism and timing belt parts on the MTZ-82 tractor (sample No. 2) twice a year (during seasonal maintenance), it is possible to completely clean the crank mechanism and timing belt parts of a diesel engine from carbon deposits in-place method and increase the average piston compression in the cylinders by 15.3%, and reduce the unevenness of compression in the cylinders by 21%.

CONCLUSION

It is preferable to use a technical fluid (water), which is supplied to the combustion chamber of a diesel engine, by microwave action of the vapor-air mixture with the surface of carbon deposits, which it cleans. Where it is possible to completely clean the crankshaft mechanism and timing belt parts of a diesel engine from carbon deposits in a localized manner and increase the average piston pressure in the cylinders by 15.3% and reduce the unevenness of compression in the cylinders by 21% twice a year (during seasonal maintenance). And Combustion of the fuel-steam-air mixture in the combustion chamber allows not only to remove the formed carbon deposits, but also to prevent their further formation. Incorporating magnetite nanoparticles into the base diesel (0/25/50 ppm) under steam co-injection delivered a consistent emissions benefit without hardware changes. Across the operating map, Fe_3O_4 lowered exhaust soot, with the largest gains at moderate steam fractions (K_Prvc 12–23%), while specific fuel consumption improved slightly (1–2%) and effective power remained within repeatability. Endurance checks indicated cleaner injector tips and thinner in-cylinder deposits; no stability issues or abnormal filter loading were observed when blends were pre-filtered through 10 µm elements. Taken together, the data point to a practical operating window K_Prvc 12–18% with 50 ppm Fe_3O_4 at 1300–1500 min^{-1}, mid rack that jointly suppresses soot and trims SFC without sacrificing power. Because the approach is drop-in, it can be adopted alongside existing steam systems with minimal integration effort. Two limitations should guide follow-up work: particle-number emissions and long-term ash management were not quantified here. Future studies should track PN, characterize ash accumulation in after-treatment components, extend durability to longer duty cycles, and compare Fe-based additives with alternative nanoparticle chemistries and doses.

CONFLICT OF INTEREST

The authors declare that there is no conflict of interests regarding the publication of this manuscript.

REFERENCES

1. Maidi A, et al. Mathematical Modeling of Thermo-Regulation of Fuel In Diesel Engines Yamz-238*. Iraqi Journal of Agricultural Sciences. 2018;49(4).
2. Al-Maidi AAH, Al Tameemi KAK, Al-Maidi AAH. Environmental Solutions and Economic Benefits for Using Natural Gas in Agricultural Engines. Misan Journal of Agricultural and Environmental Sciences. 2025;1(1):17-27.
3. Al-Maidi AAH, Chernetsov DA. Analysis of Results of Research of Fuel System of Yamz-238 Engine Operating Gas Diesel Cycle. Chronos Journal. 2020(1(40)).
4. Fahad Resan Sa, Jasim NA. Experimental and Numerical Investigation of Aluminum Beams: Flexural Behavior Section Shape Effect. Misan Journal of Engineering Sciences. 2022;1(2):37-49.
5. L. Saleh A, Altai HDS, Lazim MH, Hazim HT, Lpizra A. Solving Unit Commitment Including Wind Power Generation Using PSS®E. Misan Journal of Engineering Sciences. 2022;1(1):69-93.
6. Hussein AR, Dakhil AM, Rashed JR, Othman MF. Intelligent Expert System for Diagnosing Faults and Assessing Quality of Power Transformer Insulation Oil by DGA Method. Misan Journal of Engineering Sciences. 2022;1(1):47-57.
7. Rodionov Y, Lomovskikh A, Abasov M, Kazakevich D, Kiselyov M, Rybin G. A Method and Device for Improving the Performance of Diesel Engines of Agricultural Machinery Removed from Warranty. Science In The Central Russia. 2025(2):119-133.
8. Kalinichenko A, Hruban V, Marchenko D. Promising

Approaches for Heat Utilization in Agricultural Machinery Engines. Applied Sciences. 2024;14(19):8717.
9. Wang X, Li J, Jia X, Ma M, Ren Y. Characterization of Carbonaceous Deposits on an End-of-Life Engines for Effective Cleaning for Remanufacturing. Sustainability. 2021;13(2):950.
10. Rodionov Y, Agafonov A, Lomovskikh A, Berestevich G, Sever A, Rybin G. Technology of Non-Selective Restoration and Prolongation of the Life of Parts and Mechanisms of Power Plants of Agricultural Machinery. Science in the Central Russia. 2023(6):111-122.
11. Weidenlener A, Pfeil J, Kubach H, Koch T, Forooghi P, Frohnapfel B, et al. The influence of operating conditions on combustion chamber deposit surface structure, deposit thickness and thermal properties. Automotive and Engine Technology. 2018;3(3-4):111-127.
12. Rodionov Y, Danilin S, Lomovskih A, Sever A, Kiselev M, Rybin G. Method Of Increasing The Technical And Operational Properties of Agricultural Machinery Samples. Science in the Central Russia. 2024(6):19-33.
13. Kokieva G, Krivoshapkin K, Dondokov Y, Evseeva M, Stroyev A. The role and improvement of technical services in agriculture. E3S Web of Conferences. 2021;273:07006.
14. Grimaldi CN, Millo F. Internal Combustion Engine (ICE) Fundamentals. Handbook of Clean Energy Systems: Wiley; 2015. p. 1-32.
15. Anand G, Ravi MR, Subrahmanyam JP. Performance and Emissions of Natural Gas and Hydrogen/Natural Gas Blended Fuels in Spark Ignition Engine. ASME 2005 Internal Combustion Engine Division Spring Technical Conference; 2005/01/01: ASMEDC; 2005. p. 337-341.
16. Dec JE. A Conceptual Model of DI Diesel Combustion Based on Laser-Sheet Imaging*. SAE Technical Paper Series; 1997/02/24: SAE International; 1997.
17. Rakopoulos CD, Giakoumis EG. Simulation and exergy analysis of transient diesel-engine operation. Energy. 1997;22(9):875-885.
18. Sadhik Basha J, Anand RB. Role of nanoadditive blended biodiesel emulsion fuel on the working characteristics of a diesel engine. Journal of Renewable and Sustainable Energy. 2011;3(2).
19. Sajith V, Sobhan CB, Peterson GP. Experimental Investigations on the Effects of Cerium Oxide Nanoparticle Fuel Additives on Biodiesel. Advances in Mechanical Engineering. 2010;2.
20. Jung H, Kittelson DB, Zachariah MR. The influence of a cerium additive on ultrafine diesel particle emissions and kinetics of oxidation. Combust Flame. 2005;142(3):276-288.
21. Stanmore BR, Brilhac JF, Gilot P. The oxidation of soot: a review of experiments, mechanisms and models. Carbon. 2001;39(15):2247-2268.
22. Zhou Y, He Q, Sha Y, Shen C, You X. Effects of ferrocene addition on soot formation characteristics in laminar premixed burner-stabilized stagnation ethylene flames. J Aerosol Sci. 2024;175:106265.
23. Tkachenko YL, Morozov SD, Sherbakova IS, Rovnyagina AS. Why we need to purify the air from carbon dioxide. IOP Conference Series: Earth and Environmental Science. 2021;815(1):012006.
24. Kökkülünk G, Parlak A, Ayhan V, Cesur İ, Gonca G, Boru B. Theoretical and experimental investigation of steam injected diesel engine with EGR. Energy. 2014;74:331-339.
25. Hajiyeva A, Mammadova U, Tanriverdiyeva G, Kovalenko O. Technological innovations in agriculture: Impact on production efficiency. Scientific Horizons. 2023;27(1):172-182.
26. Reckitt patents cleaning system. Focus on Surfactants. 2010;2010(7):5.
27. Gontar LO. ЗАЩИТА ПЕРСОНАЛЬНЫХ ДАННЫХ В УСЛОВИЯХ РАЗВИТИЯ ИНТЕРНЕТ- КОМПАНИЙ: МЕЖДУНАРОДНО-ПРАВОВОЕ РЕГУЛИРОВАНИЕ VS САМОРЕГУЛИРОВАНИЕ. Труды по Интеллектуальной Собственности. 2021;37(1-2):116-140.
28. Instrumentation for recording the operating data of supercharged engines on the engine test bench. Powertrain: Springer Vienna. p. 184-193. http://dx.doi.org/10.1007/978-3-211-47113-5_10
29. Басиладзе СГ. МЕТОДЫ СЧИТЫВАНИЯ, СБОРА И ПЕРЕДАЧИ ДАННЫХ В УСТАНОВКАХ ЯДЕРНО-ФИЗИЧЕСКОГО ЭКСПЕРИМЕНТА , «Приборы и техника эксперимента». Приборы и техника эксперимента. 2017(5):5-73.
30. Mashkov S, Ishkin P, Zhiltsov S, Mastepanenko M. Methods of determining the need for agricultural machinery. IOP Conference Series: Earth and Environmental Science. 2019;403(1):012079.
31. Prohorenko A, Dumenko P. Software Algorithm Synthesis for Diesel Electronic Control Unit. Latvian Journal of Physics and Technical Sciences. 2018;55(3):16-26.